Efficient Beam Search For Satellite Communications On The Move Systems

Ziping Wei, Yongchun Chen, Kaiqi Guo, Bingsen Liu, Yue Liu, Yihuan Li

***Abstract*—Satellite Communication on the Move (SOTM) is critical for operations requiring mobility. Conventional approaches employing parabolic reflector antennas exhibit limitations, including sluggish mechanical scanning speeds and suboptimal tracking efficiency, particularly for Low Earth Orbit (LEO) satellites. In contrast, phased array antennas offer faster and more accurate tracking but are still underutilized in practical SOTM systems. A fundamental obstacle is ensuring precise beam alignment between satellites and mobile terminals, it would affects the tracking performance. However, many existing beam alignment methods are computationally intensive and unsuitable for real-time applications. This study introduces a computationally efficient beam alignment algorithm capitalizing on the inherent rank-restricted structure of our constructed beamspace matrix. The alignment task is formulated as a non-convex maximization problem, and a randomized matrix approximation is employed to construct the beamspace. This enables the extraction of a subspace likely to contain the optimal value. Particle Swarm Optimization (PSO) is subsequently applied within this subspace to iteratively refine the beam estimate. Numerical simulations demonstrate that the proposed method improves beam search accuracy by an order of magnitude and reduces computational cost by over $> 60\%$ compared to existing approaches. This advancement offers significant potential for enhancing SOTM system performance in highly dynamic environments.**

***Index Terms*—Satellite communication, SOTM, Beam alignment, PSO.**

I. Introduction

SATELLITE communication is expected to play a pivotal role in future 6G mobile networks, serving as a global relay to enable high-speed, seamless, and ubiquitous broadband connectivity. Among its emerging applications, Satellite Communication on the Move (SOTM) has gained increasing significance by facilitating stable and reliable satellite links for mobile platforms—such as ships, aircraft, and ground vehicles—in motion. The technology has attracted widespread adoption due to its critical role in mission-critical scenarios, including military operations, emergency response, maritime communications, and bridging the digital divide in remote or underserved regions.

However, the deployment of SOTM systems faces inherent limitations when relying on mechanically steered parabolic reflector antennas, particularly in Low Earth Orbit (LEO) scenarios. The slow scanning speed and suboptimal tracking efficiency of these antennas significantly limit system performance [1], [2]. In contrast, electronically steered phased arrays offer a promising solution by enabling agile beam steering through phase shifters [3]. Despite their potential, practical implementation remains challenged by unresolved issues in beam alignment accuracy and dynamic tracking under high-mobility conditions.

Establishing robust SOTM links critically depends on precise initial beam alignment [4], which is a prerequisite for maintaining continuous connectivity under platform mobility. Conventional solutions rely on sensor fusion of Global Navigation Satellite System (GNSS), compasses, and Inertial Measurement Unit (IMU) for attitude estimation [5], but these approaches suffer from cumulative errors in low-cost sensors, often resulting in beam misalignment and signal degradation.

To address these limitations, several dominant methodological paradigms have emerged, each targeting specific aspects of the alignment problem with associated limitations. Classical brute-force beam sweeping offers simplicity but incurs excessive time and computational overhead. Hierarchical codebook approaches reduce training complexity, yet they perform poorly in dynamic environments [6]. High-resolution Direction-of-Arrival (DOA) estimators (e.g., MUSIC [7]) provide high accuracy at the expense of increased computational load. Hybrid inertial-electronic tracking methods [8] improve robustness but remain sensitive to sensor fusion stability. Stochastic optimization techniques (e.g., Particle Swarm Optimization (PSO) [9], [10]) effectively balance exploration and exploitation, yet scale poorly in real-time systems. Despite their respective advantages, all existing approaches exhibit fundamental trade-offs among alignment accuracy, latency, and adaptability—particularly in high-mobility SOTM scenarios where computational efficiency becomes critical.

Recently, an active phased array antenna specifically designed for direct broadcast satellite (DBS) is developed to improve the beam alignment efficiency [11]. This architecture leverages advanced array processing to improve satellite signal acquisition while reducing the number of active and control

Manuscript received December 23, 2024; revised July 10, 2025.

Ziping Wei is an engineer of Satellite technology & Application Research Institute of China Telecom Corporation Limited, Beijing, 100032, China (corresponding author to provide phone: +86 17778071126, e-mail: weizp.wx@chinatelecom.cn).

Yongchun Chen is an senior engineer of Satellite technology & Application Research Institute of China Telecom Corporation Limited, Beijing, 100032, China (e-mail: chenych@chinatelecom.cn).

Kaiqi Guo is an engineer of Satellite technology & Application Research Institute of China Telecom Corporation Limited, Beijing, 100032, China (e-mail: gkq.wx@chinatelecom.cn).

Bingsen Liu is an engineer of Satellite technology & Application Research Institute of China Telecom Corporation Limited, Beijing, 100032, China (e-mail:liubingsen@chinatelecom.cn).

Yue Liu is an senior engineer of Satellite technology & Application Research Institute of China Telecom Corporation Limited, Beijing, 100032, China (e-mail: liuyue@chinatelecom.cn).

Yihuan Li is an senior engineer of Satellite technology & Application Research Institute of China Telecom Corporation Limited, Beijing, 100032, China (e-mail: liyihuan@chinatelecom.cn).

components. Concurrently, ref. [8] proposes a hybrid tracking strategy that integrates inertial yaw rate sensor data with electronic feedback from the antenna system, enabling high-precision beam alignment.

We propose a computationally efficient beam alignment framework which uses the low-rank property of such beamspace matrices. Specifically, the beam alignment process is constructed as a novel problem with several non-convex constraints. To address such problem, we reconstruct a low-rank beamspace matrix via randomized approximation techniques. Then, an attention subspace that encapsulates the optimum is obtained and PSO algorithm is employed to estimate the target direction. Compared to conventional approaches, specifically exhaustive beam search and canonical PSO, our method achieves $> 60\%$ reduction in computational complexity and an 8 speedup ratio over canonical methods, significantly enhancing real-time performance in SOTM systems. The main contributions are summarized as following:

1) We analyze the beam alignment process, and formulate it as an innovative optimization problem. This formulation addresses previously unresolved challenges in optimization theory specific to dynamic satellite communication scenarios.

2) We develop an novel beam search method that leverages randomized matrix approximation techniques. This approach enables high-precision estimation of both azimuth and elevation information for terminal beam search, while reducing time complexity by several orders of magnitude compared to state-of-the-art methods. To further optimize practical implementation, we introduce a computationally efficient sampled length estimation algorithm that dynamically adapts to system constraints.

3) Comprehensive computational complexity analysis of our developed algorithm is provided, and it is supported by extensive numerical simulations. The results demonstrate that our method achieves high accuracy while maintaining computational requirements that are suitable for real-time operation, making it particularly well-suited for widespread deployment in SOTM applications.

II. System Model

This work focuses on the GEO satellite-to-SOTM communication link. The GEO satellite operates at the standard altitude of 35,786 km (see Fig. 1). The mobile SOTM terminal employs a Uniform Planar Array (UPA) with dimensions $M_x \times M_y$. Following the model in [12], the channel matrix $\mathbf{H} \in \mathbb{C}^{M_x \times M_y}$ between the GEO satellite and the satellite terminal at instant time t and frequency f is characterized by:

$$\mathbf{H}(t,f) = \sum_{l=0}^{L_k-1} G_l \exp\left[j2\pi(tv_l - f\tau_l)\right]\mathbf{V}_l(\alpha_l,\beta_l), \quad (1)$$

where L_k is the number of propagation paths. G_l represents the complex channel gain for the l_{th} path. The UPA's array response matrix $\mathbf{V}_l$ for the l_{th} path, parameterized by the azimuth angle and elevation angle, has its (m,n) element defined as:

$$\mathbf{V}_l\left(\alpha_l,\beta_l\right) = e^{j\frac{2\pi d}{\lambda}[(m_x-1)\sin\alpha_l\cos\beta_l+(m_y-1)\sin\alpha_l\sin\beta_l]}; \quad (2)$$

Here, d is the inter-element spacing and λ is the carrier wavelength. The composite channel gain G_l aggregates several loss components [13]:

$$G_l = P_{L_{dl1}} + P_{L_{da1}} + P_{L_{dp1}} + P_{L_{ds1}}. \quad (3)$$

Specifically, $P_{L_{dl1}}$ is the free-space path loss, incorporating shadow fading and clutter loss. $P_{L_{da1}}$ is the Atmospheric attenuation losses; $P_{L_{dp}}$ is the building penetration loss (where applicable); $P_{L_{ds}}$ is the miscellaneous losses from unmodeled factors.

Consequently, the received signal vector at the SOTM terminal is:

$$\mathbf{y} = \mathbf{w}^H\mathbf{h}\mathbf{s} + \mathbf{w}^H\mathbf{n}. \quad (4)$$

In this expression, $\mathbf{s}$ is the transmitted signal symbol, $\mathbf{h} = vec(\mathbf{H}) \in \mathbb{C}^{M_xM_y\times 1}$ is the vectorized channel, $\mathbf{n}$ is the additive noise vector, $\mathbf{w} \in \mathbb{C}^{M_xM_y\times 1}$ is the beamforming vector.

III. Efficient Beam Alignment Algorithm

In this section, the original non-convex problem is reformulated, and an efficient beam search algorithm is developed to achieve high-precision beam direction estimation. In addition, the computational complexity of the proposed approach is thoroughly analyzed.

A. Problem Reformulation

The instantaneous received signal energy at the SOTM terminal can be computed for any given beamforming vector $\mathbf{w}(\alpha_0,\beta_0)$ with unit norm ($\|\mathbf{w}\| = 1$), as follows:

$$\begin{aligned}\Omega_0 &= \|\mathbf{y}\|_2^2 = \mathbf{y}\mathbf{y}^H \\ &= \mathbf{w}(\alpha_0,\beta_0)^H\mathbf{R}_1\mathbf{w}(\alpha_0,\beta_0) + \mathbf{w}(\alpha_0,\beta_0)^H\mathbf{R}_2\mathbf{w}(\alpha_0,\beta_0),\end{aligned} \quad (5)$$

where $\mathbf{R}_1 = \mathbf{h}\mathbf{s}\mathbf{s}^H\mathbf{h}^H$ and $\mathbf{R}_2 = \mathbb{E}[\mathbf{n}\mathbf{n}^H]$ denote the signal and noise covariance matrices, respectively.

It is evident that the received signal energy Ω_0 varies with the beamforming vector $\mathbf{w}(\alpha_0,\beta_0)$. This leads to the following optimization problem for maximizing the received power:

$$\max_{\mathbf{w}} \left\|\mathbf{w}^H\mathbf{R}_1\mathbf{w} + \mathbf{w}^H\mathbf{R}_2\mathbf{w}\right\|_F^2, \quad \text{s.t.} \quad \|\mathbf{w}\| = 1. \quad (6)$$

Following established beamforming theory [5], the ideal receive vector that maximizes directional alignment with the target satellite is expressed as $\mathbf{w} = \mathrm{vec}(\mathbf{V}(\alpha,\beta))$. This formulation enables precise beam steering toward the satellite's transmission direction. The parameters α and β in this expression correspond to the transformed azimuth and elevation angles, respectively, describing the satellite's relative position in the terminal's coordinate frame.

As observed, the estimation accuracy of α and β directly affects the initial beam alignment performance. However, conventional methods such as classical DOA estimation or exhaustive beam sweeping typically incur high computational complexity.

Specifically, classical beam search method involves scanning over all possible beam directions in the azimuth-elevation domain ($\alpha \in [0, 2\pi], \beta \in [-\pi/2, \pi/2]$) to identify the optimal

beam pair. This process can be formulated as the following optimization problem:

$$\begin{aligned} &\arg\max_{(\alpha,\beta)} \quad \mathbf{F}(\alpha,\beta) \\ &\text{s.t.} \quad \begin{cases} \mathbf{F}(\alpha,\beta) = \left\| \mathbf{w}^H \mathbf{R}_1 \mathbf{w} + \mathbf{w}^H \mathbf{R}_2 \mathbf{w} \right\|, \\ \alpha \in \{\alpha_0 \mid \alpha_0 \in [0, 2\pi]\}, \\ \beta \in \left\{\beta_0 \mid \beta_0 \in [0, \frac{\pi}{2}]\right\}, \\ \|\mathbf{w}(\alpha,\beta)\| = 1. \end{cases} \end{aligned} \tag{7}$$

In this context, $\mathbf{F}(\alpha,\beta) \in \mathbb{C}^{M\times N}$ denotes the two-dimensional discrete problem space matrix. Traditional beam sweeping methods require extensive sampling to explore $\mathbf{F}(\alpha,\beta)$ and locate its maximum value [14]. Moreover, both the estimation accuracy and computational complexity are closely related to the chosen sweeping interval.

Let the azimuth and elevation sweeping intervals be $\Delta\alpha = 2\pi/M$ and $\Delta\beta = \pi/N$, respectively. The size of the search space becomes $\mathbf{F} \in \mathbb{C}^{M\times N}$, and the total number of beam sweeping operations required is $M \times N$.

This exhaustive search approach, although conceptually straightforward, introduces significant overhead in terms of time and computational resources, especially when high-resolution beam alignment is required.

B. Efficient Beam Search

1) Low-Rank Problem Space Representation: To achieve dimensionality reduction without compromising estimation accuracy, our methodology employs a low-rank reconstruction paradigm. We first define the azimuth and elevation scanning vectors $\mathbf{p}_1 \in \mathbb{R}^M$ and $\mathbf{q}_1 \in \mathbb{R}^N$ through angular domain discretization:

$$\mathbf{p}_s = [0, 2\pi/M, ..., 2\pi] \in \mathbb{R}^M, \tag{8a}$$

$$\mathbf{q}_s = [0, \pi/2N, ..., \pi/2] \in \mathbb{R}^N. \tag{8b}$$

We then construct the compressed sub-vector $\mathbf{q}_s(\mathcal{J}_1)$ through uniform downsampling of the elevation vector $\mathbf{q}_s$, selecting exactly $\lfloor s/2 \rfloor$ elements according to the following representation:

$$\mathbf{q}_s(\mathcal{J}_1) \in \mathbb{R}^{s/2}, \mathcal{J}_1 = [j_1, j_2, ..., j_{s/2}]. \tag{9}$$

The index set $\mathcal{J}_1 \subseteq 1, 2, \ldots, M$ is generated through uniform sampling. The sampling length s satisfies $\text{rank}(\mathbf{F}) \leq s \ll \min(M, N)$, where s is functionally dependent on the matrix rank and can be approximated using established methods [14].

We then perform a dual-vector traversal over $\mathbf{p}_s$ and the compressed elevation vector $\mathbf{q}_s(\mathcal{J}_1)$, dynamically updating the SOTM beam configuration during sampling. This procedure constructs the partial observation matrix $\mathbf{F}_{fro} = \mathbf{F}(\mathbf{p}_s, \mathbf{q}_s(\mathcal{J}_1)) \in \mathbb{C}^{M\times s/2}$.

Column variance analysis of $\mathbf{F}_{\text{fro}}$ identifies the dominant s column indices, denoted $\mathcal{I}$. Mirroring this approach, we generate the complementary sub-matrix $\mathbf{F}_r$ by traversing the reduced azimuth vector $\mathbf{p}_1 = \mathbf{p}_s(\mathcal{I})$ against the full elevation vector $\mathbf{q}_s$, while simultaneously adjusting beam alignment. The column-space representation $\mathbf{F}_r$ admits the theoretical formulation:

$$\mathbf{F}_r = \mathbf{F}(\mathbf{p}_1, \mathbf{q}_s) \in \mathbb{C}^{s\times N}. \tag{10}$$

We compute row-wise variance metrics for the column-submatrix $\mathbf{F}_c \in \mathbb{C}^{M\times s}$, identifying the index set $\mathcal{J}_2$ corresponding to the $\lfloor s/2 \rfloor$ most significant variance values. Applying the established beam adjustment procedure to the parameter pair $\mathbf{p}_s$ and $\mathbf{q}_s(\mathcal{J}2)$ yields a secondary partial matrix $\mathbf{F}_{fro2}$. Consequently, the row-submatrix $\mathbf{F}_r$ is derived through the relationship:

$$\mathbf{F}_r = [\mathbf{F}_{fro}; \mathbf{F}_{fro2}] = \mathbf{F}(\mathbf{p}_s, \mathbf{q}_1), \mathbf{q}_1 = [\mathbf{q}_s(\mathcal{J}_1); \mathbf{q}_s(\mathcal{J}_2)]. \tag{11}$$

The theoretical intersection between the column-submatrix $\mathbf{F}_c$ and row-submatrix $\mathbf{F}_r$ constitutes the core submatrix $\mathbf{F}_u$ = $\mathbf{F}(\mathbf{p}_1, \mathbf{q}_1) = \mathbf{F}_c(:, \mathbf{q}_1) = \mathbf{F}_r(\mathbf{p}_1 :,) \in \mathbb{C}^{s\times s}$. Leveraging randomized matrix approximation techniques [14], [15], we reconstruct the original $M \times N$ problem space matrix through the factorized representation:

$$\hat{\mathbf{F}} = \mathbf{F}_c \mathbf{W} \mathbf{F}_r, \mathbf{W} = (\mathbf{F}_u)^\dagger = \mathbf{F}_c(:, \mathbf{q}_1)^\dagger, \tag{12}$$

where $\mathbf{W}$ is a weighting matrix computed using the Moore-Penrose pseudo-inverse. The resulting $\hat{\mathbf{F}}$ represents the reconstructed low-rank approximation of $\mathbf{F}$. As established in [15], [16], the approximation error $|\mathbf{F} - \hat{\mathbf{F}}|$ admits a theoretical bound proportional to the sampling complexity parameter $(M + N)s - s^2$:

$$\sum_{i=s+1}^{\min(M,N)} \sigma_i^2 \leq \|\mathbf{F} - \mathbf{F}_c \mathbf{W} \mathbf{F}_r\| \leq (1 + \xi) \sum_{i=s+1}^{\min(M,N)} \sigma_i^2, \tag{13}$$

where σ_i is the i_{th} singular value of $\mathbf{F}$; $\xi \in [0, 1]$ is one parameter related to s.

Therefore, it only required $[(M + N)s - s^2]$ samples to construct the space matrix $\mathbf{F}$ by our method.

2) Evolutionary Search: Based on the above recovered matrix $\hat{\mathbf{F}}$, we then obtain the attention subspace, which contain the optimum [14]:

$$\mathcal{O} = \{\hat{\alpha}_1 - \frac{2\pi}{M} < x < \hat{\alpha}_1 + \frac{2\pi}{M}, \hat{\beta}_1 - \frac{\pi}{2N} < y < \hat{\beta} + \frac{\pi}{2N}\}. \tag{14}$$

Here, $\langle \hat{\alpha}_1, \hat{\beta}_1 \rangle$ is the maximum of $\hat{\mathbf{F}}$. i.e.,

$$\langle \hat{\alpha}_1, \hat{\beta}_1 \rangle = \arg\max(\hat{\mathbf{F}}). \tag{15}$$

The conventional PSO is subsequently applied to explore the compact attention subspace $\mathcal{O}$. For initialization, K particles are generated through uniform random sampling within attention subspace. After T generations, the algorithm yields optimal azimuth-elevation angle estimates $\langle \hat{\alpha}, \hat{\beta} \rangle$ [17], [18].

C. Sampled Length Estimation

To facilitate the practical deployment of the proposed beam search algorithm, it is crucial to estimate an appropriate sampling length s for the problem space matrix $\mathbf{F}$. In this section, we develop a low-complexity estimation strategy that accurately determines the optimal sampling length s. The method proceeds in two iterative steps.

Step 1: Sub-matrix Construction. At each iteration i, we set the current sampling length as $s = s_i$ ($s_i > 1$), and

Algorithm 1 Proposed Beam Search

Input: Matrix size M, N, K, T
Output: $\hat{\alpha}$, $\hat{\beta}$.

```
p_s, q_s, s = s_i, i = 0;
While Σ_{k=l_i+1}^{s_0} μ_k < μ_{l_i}, do
Randomly sampling the p_s, q_s(J_{1,i}).
Constructing F_fro = F(p_s, q_s(J_{1,i})), and select the I_i via the column variance.
Constructing F_ri = F(p_s(I_i), q) ∈ C^{s×N}, and selecting the J_{2,i}.
Constructing F_fro2 = F(p, q(J_{2,i})), F_ci = [F_fro; F_fro2].
F̂_i according to eq. (12).
F̂_i = U_i diag([μ_1, μ_2, ..., μ_{s_i}])V_i via SVD.
s_i = s_i + 1.
End While.
Obtaining the O.
Applying the PSO algorithm based on K, O and T.
Obtaining ⟨α̂, β̂⟩.
```

construct two submatrices $\mathbf{F}_{ci}, \mathbf{F}_{ri}$ based on the column and row selection criteria detailed in Section III-B. Subsequently, a low-rank approximation matrix is computed as:

$$\hat{\mathbf{F}}_i = \mathbf{F}_{ci} \left(\mathbf{F}_{ci}(:, \mathbf{q}_i) \right)^{\dagger} \mathbf{F}_{ri}, \tag{16}$$

where $(\cdot)^{\dagger}$ denotes the Moore–Penrose pseudoinverse, and $\mathbf{q}_i$ represents the selected column indices at the i-th iteration.

Step 2: Singular Value Residual Analysis. Next, we perform singular value decomposition (SVD) on $\hat{\mathbf{F}}_i$, which yields:

$$\hat{\mathbf{F}}_i = \mathbf{U}_i \, \mathrm{diag}\left([\mu_1, \mu_2, \ldots, \mu_{s_i}] \right) \mathbf{V}_i^H, \tag{17}$$

where μ_k denotes the k-th singular value.

The sampling length s is then estimated by evaluating the residual energy of the singular values. Specifically, the estimated rank is determined once the following condition is satisfied:

$$\sum_{k=l_i+1}^{s_i} \mu_k < \mu_{l_i}. \tag{18}$$

If no such l_i exists for the current s_i, the sampling length is incremented as $s_i = s_i + 1$, and the SVD step is repeated with the updated submatrices. This iterative process continues until the above stopping criterion in eq. (16) is met or the maximum number of iterations $t_{\max}$ is reached.

The reconstruction error between the final approximated matrix $\hat{\mathbf{F}}_{\max}$ and the original matrix $\mathbf{F}$ is theoretically bounded as analyzed in eq. (13). The complete procedure is summarized in **Algorithm 1**.

D. Complexity Analysis

This section presents the time complexity analysis of the proposed efficient beam search algorithm. As outlined in the algorithmic framework, the computational burden of the proposed method primarily consists of two major components: (1) beam direction optimization and (2) matrix operations.

First, the beam direction optimization process in the SOTM system involves $t_1[(M+N)s - s^2 + TK]$ sequential adjustments. Assuming each directional adjustment cycle requires t_1 seconds, the total execution time for this phase is given by:

$$T_{\text{beam}} = t_1 \left[(M+N)s - s^2 + TK \right]. \tag{19}$$

Second, the algorithm incorporates several sophisticated matrix computations, including singular value decomposition (SVD), matrix inversion, and matrix multiplication. Among these, the computational complexity is dominated by the matrix multiplication operations, which collectively involve:

$$\mathcal{O}\left(t_{\max} \left(Ms^2 + sMN + 2s^3 \right) \right) \tag{20}$$

arithmetic operations.

Accordingly, the upper bound on the execution time for the matrix computation stage can be expressed as:

$$T_{\text{matrix}} = t_2 \cdot t_{\max} \left(Ms^2 + sMN + 2s^3 \right), \tag{21}$$

where t_2 denotes the average time required for a single multiplication operation.

Finally, combining both components, the overall time complexity of the proposed algorithm is derived as:

$$t_1 \left[(M+N)s - s^2 + TK \right] + t_2 t_{\max} \left(Ms^2 + sMN + 2s^3 \right). \tag{22}$$

As analyzed, the complexity of multiplication process in our method almost can be negligible, when comparing to the beam search complexity. This analytical model provides a comprehensive characterization of the computational efficiency of the proposed beam alignment strategy.

IV. Simulation Results

In this section, we now provides comprehensive validations. To establish rigorous performance baselines, we systematically benchmark our method against five state-of-the-art beam alignment paradigms spanning classical to recent advances: 1) Stochastic optimizers (Canonical PSO [9]), 2) Subspace estimators (MUSIC), 3) Exhaustive search, 4) Hierarchical search [6], 5) Hybrid switching (BSA [19]). This selection covers all dominant signal processing strategies, from computationally intensive high-precision methods to real-time heuristics, providing exhaustive coverage of the SOTM beam alignment design space.

A. Simulation Parameters

In the simulation setup, the target satellite is positioned in geostationary orbit at a longitude of $134°$E, while the SOTM is located at $130°$E and $30°$N. The key simulation parameters are summarized as follows: 1) The satellite-to-terminal communication operates in the Ku-band at a carrier frequency of $14.25,$GHz; 2) The uniform planar array (UPA) has an inter-element spacing of $d = 0.5\lambda$; 3) The effective isotropic radiated power (EIRP) of the satellite is set to 50dBW; 4) The antenna gain-to-noise-temperature ratio (G/T) of the SOTM terminal is specified as 2dB/K; 5) The array dimensions are $M_x = M_y = 16$, resulting in a total of $M = 361$ elements; 6) The search space is characterized by parameters $N = 91$, $K = 20$, $T = 20$, and $s = 6$.

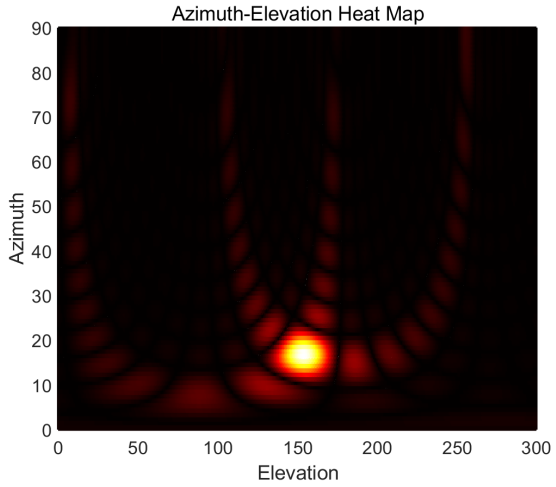

(a) The original problem space matrix

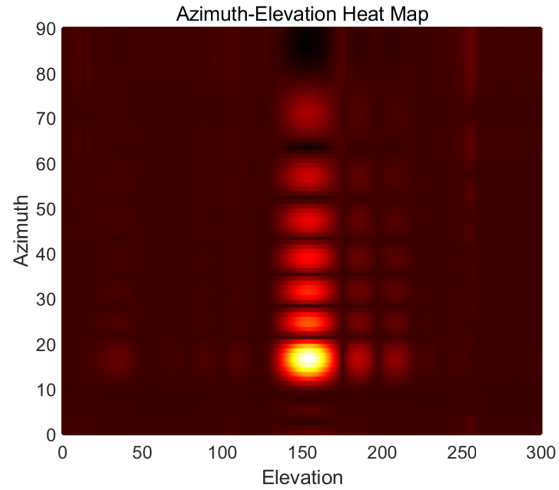

(b) The reconstructed problem space matrix

Fig. 1: Recovered attention subspace.

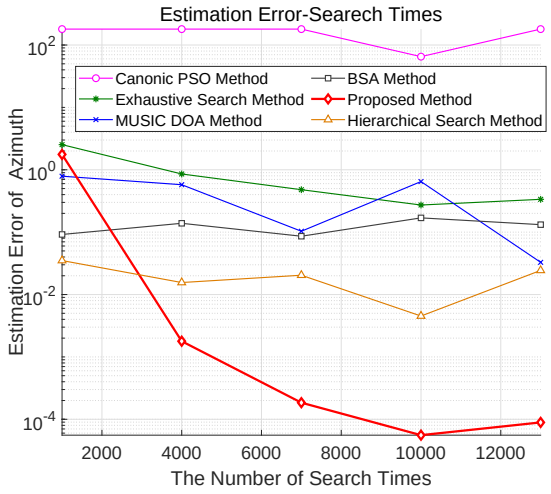

(a) Azimuth estimation performance

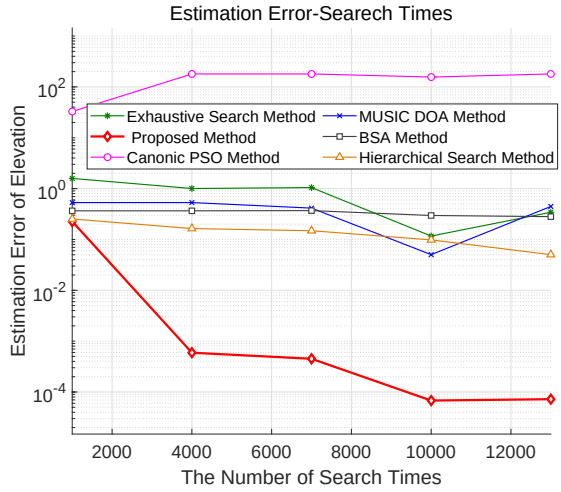

(b) Elevation estimation performance

Fig. 2: Different algorithms estimation performance varies with the number of beam searches times.

B. Problem Space Reconstruction

We first assess the reconstruction accuracy of the problem space matrix $\hat{\mathbf{F}}$ generated by our algorithm, in comparison to the ground-truth matrix $\mathbf{F}$. Fig. 2(a) shows the original matrix $\mathbf{F}$, computed via exhaustive traversal over discretized elevation and azimuth angles (horizontal and vertical axes, respectively). Fig. 2(b) depicts the reconstructed matrix $\hat{\mathbf{F}}$ along with the attention subspace $\mathcal{O}$ identified by our method. As illustrated, the proposed algorithm reconstructs $\mathbf{F}$ with high fidelity, and the identified subspace $\mathcal{O}$ reliably encloses the optimal solution to problem (7). Importantly, this reconstruction requires only $[(M+N)s - s^2] = 2676$ beam search operations, significantly fewer than the $MN = 32851$ required for exhaustive search (i.e., $[(M+N)s - s^2] \ll MN$).

C. Angle Estimation Accuracy

We evaluate the accuracy of elevation and azimuth angle estimation achieved by our method against five state-of-the-art techniques: Canonical PSO, MUSIC, Exhaustive Search, Hierarchical Search, and BSA [5], [7], [19]. Fig. 3(a) and 3(b) present the estimation errors as a function of the number of beam searches, where the horizontal axis denotes beam search count, and the vertical axis represents the angular error (i.e., the deviation between the true and estimated angles). As shown in the Fig. 3(a) and (b), our proposed method consistently achieves the lowest estimation error across all beam search budgets. Moreover, with increased beam search count, the elevation and azimuth errors decrease rapidly, yielding a final estimation accuracy improvement of 20%-40% over other approaches.

D. Algorithm Scalability

To validate scalability, we examine the performance of our method under varying UPA configurations. Fig. 4(a) and 4(b) show the angle estimation errors across different array sizes, denoted by $< M_x, M_y >$. The horizontal axis reflects the number of array elements, while the vertical axis shows the corresponding estimation error. As demonstrated, the pro-

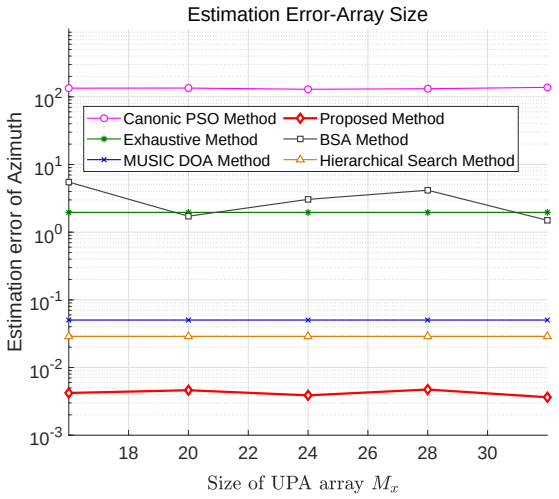

(a) Azimuth estimation performance

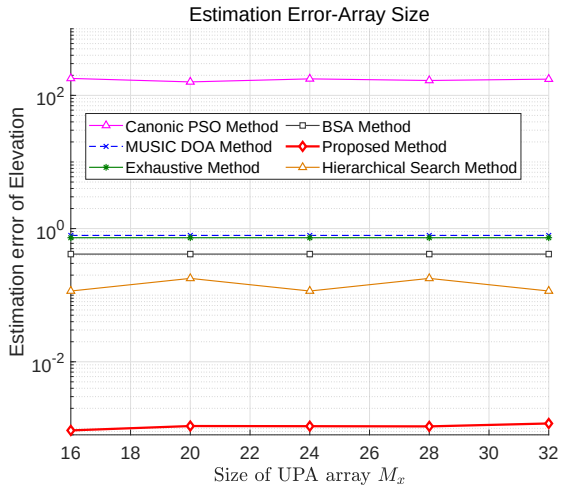

(b) Elevation estimation performance

Fig. 3: Different algorithms estimation performance varies with the size of UPA array antenna.

posed algorithm maintains robust accuracy across all tested configurations ($M_x, M_y \in [16, 32]$), achieving up to a $10\times$ improvement in estimation precision compared to baseline methods for larger arrays (e.g., $M_x = M_y = 32$).

E. Computational Efficiency

We further evaluate the computational efficiency of the proposed algorithm through Monte Carlo simulations over 100 independent trials. Fig. 5 compares the CPU runtimes of different beam alignment methods across UPA configurations with $M_x \in [16, 32]$. The results reveal two key observations: First, the proposed method reduces computational overhead by more than 60% compared to conventional approaches; Second, it achieves an $8\times$ speedup over PSO-based algorithms while maintaining comparable estimation accuracy. These findings highlight the algorithms effectiveness in high-dimensional SOTM scenarios, where both computational efficiency and robust angle estimation are critical.

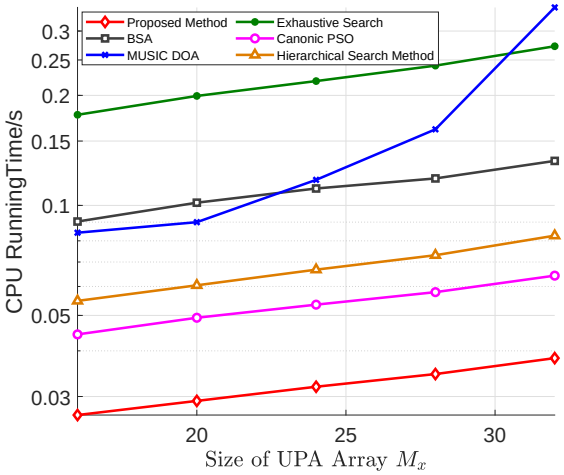

Fig. 4: CPU running time of different beam search methods across varying SOTM terminal dimensions.

V. Conclusion

This work introduces a computationally efficient beam alignment framework for SOTM systems that leverages the low-dimensional geometry of beamspace energy matrices. We recast the alignment objective as a constrained nonconvex maximization problem. Our solution employs randomized matrix approximation to construct a compressed representation of the beamspace, enabling identification of a solution-dense attention subspace. Within this reduced-dimensional space, particle swarm optimization rapidly converges to the optimal beam steering direction. Compared to conventional approaches, the proposed algorithm markedly improves alignment accuracy while substantially reducing the required complexity, making it well suited for real-time satellite communication. This method holds significant promise for advancing SOTM systems, particularly in mission-critical scenarios such as military operations, where both precision and efficiency are essential.

References

[1] S.-E. Huang, P.-H. Chang, X.-L. Lu, and J.-C. Juang, "A satcom on-the-move phased-array antenna tracking algorithm on robot operating system," 2023 23rd International Conference on Control, Automation and Systems (ICCAS), pp. 1060–1065, 2023.

[2] A. H. Aymane Ezzaim, Aziz Dahbi and A. Aqqal, "Development, implementation, and evaluation of a machine learning-based multi-factor adaptive e-learning system," IAENG International Journal of Computer Science, vol. 51, no. 9, pp. 1250–1271, 2024.

[3] O. Kodheli, E. Lagunas, N. Maturo, S. K. Sharma, B. Shankar, J. F. M. Montoya, J. C. M. Duncan, D. Spano, S. Chatzinotas, S. Kisseleff, J. Querol, L. Lei, T. X. Vu, and G. Goussetis, "Satellite communications in the new space era: A survey and future challenges," IEEE Communications Surveys & Tutorials, vol. 23, no. 1, pp. 70–109, 2021.

[4] L. Han, J. Ren, X. Ji, and G. Li, "Multi-beam satellite seeking and acquisition method for satcom-on-the-move array antenna on a high maneuverability carrier," Applied Sciences, vol. 13, no. 21, p. 11803, 2023.

[5] J. Zhao, F. Gao, Q. Wu, S. Jin, Y. Wu, and W. Jia, "Beam tracking for uav mounted satcom on-the-move with massive antenna array," IEEE Journal on Selected Areas in Communications, vol. 36, no. 2, pp. 363–375, 2018.

[6] C. Wu, C. You, Y. Liu, L. Chen, and S. Shi, "Two-stage hierarchical beam training for near-field communications," IEEE Transactions on Vehicular Technology, vol. 73, no. 2, pp. 2032–2044, 2024.

[7] M. Oh, Y.-S. Lee, J.-B. Lim, C.-O. Kang, and B. C. Jung, "Hierarchical music technique for direction finding of multiple signal sources," 2024 IEEE 21st Consumer Communications & Networking Conference (CCNC), pp. 1082–1083, 2024.
[8] H. Bolandhemmat, M. Fakharzadeh, P. Mousavi, S. H. Jamali, G. Z. Rafi, and S. Safavi-Naeini, "Active stabilization of vehicle-mounted phased-array antennas," IEEE Transactions on Vehicular Technology, vol. 58, no. 6, pp. 2638–2650, 2009.
[9] Y. Li, D. Yao, and W. Chen, "Adaptive particle swarm optimizer for beam angle selection in radiotherapy planning," IEEE International Conference Mechatronics and Automation, vol. 1, pp. 421–425, 2005.
[10] S. Gao and Y. Tian, "Research on steel surface defects detection algorithms by yolov8 based on attention mechanism," IAENG International Journal of Computer Science, vol. 51, no. 9, pp. 1309–1315, 2024.
[11] S.-I. Jeon, Y.-W. Kim, and D.-G. Oh, "A new active phased array antenna for mobile direct broadcasting satellite reception," IEEE Transactions on Broadcasting, vol. 46, no. 1, pp. 34–40, 2000.
[12] J. Heo, S. Sung, H. Lee, I. Hwang, and D. Hong, "Mimo satellite communication systems: A survey from the phy layer perspective," IEEE Communications Surveys & Tutorials, vol. 25, no. 3, pp. 1543–1570, 2023.
[13] A. Guidotti, A. Vanelli-Coralli, A. Mengali, and S. Cioni, "Non-terrestrial networks: Link budget analysis," ICC 2020-2020 IEEE International Conference on Communications (ICC), pp. 1–7, 2020.
[14] B. Li, Z. Wei, J. Wu, S. Yu, T. Zhang, C. Zhu, D. Zheng, W. Guo, C. Zhao, and J. Zhang, "Machine learning-enabled globally guaranteed evolutionary computation," Nature Machine Intelligence, vol. 5, no. 4, pp. 457–467, 2023.
[15] P. Drineas, M. W. Mahoney, and S. Muthukrishnan, "Relative-Error CUR Matrix Decompositions," SIAM Journal on Matrix Analysis and Applications, 2008.
[16] Shusen, Wang, Zhihua, and Zhang, "Improving cur matrix decomposition and the nystrm approximation via adaptive sampling." Journal of Machine Learning Research, vol. 14, pp. 2729–2769, 2013.
[17] Y. Shi and R. Eberhart, "A modified particle swarm optimizer," IEEE International Conference on Evolutionary Computation Proceedings. IEEE World Congress on Computational Intelligence (Cat. No.98TH8360), pp. 69–73, 1998.
[18] J. Nayak, H. Swapnarekha, B. Naik, G. Dhiman, and S. Vimal, "25 years of particle swarm optimization: Flourishing voyage of two decades," Archives of Computational Methods in Engineering, vol. 30, no. 3, pp. 1663–1725, 2023.
[19] B. Li, Z. Zhou, H. Zhang, and A. Nallanathan, "Efficient beamforming training for 60-ghz millimeter-wave communications: A novel numerical optimization framework," IEEE Transactions on Vehicular Technology, vol. 63, no. 2, pp. 703–717, 2013.